Enhanced NMPC for Stochastic Dynamic Systems Driven by Control Error Compensation with Entropy Optimization

Ping Zhou, *Senior Member*, *IEEE*, Xiaoyang Sun, and Tianyou Chai, *Fellow, IEEE*

Abstract—In this paper an enhanced nonlinear model predictive control (En-NMPC) method driven by control error compensation with entropy optimization and unknown state estimation is proposed for high-performance control of multivariable and non-Gaussian stochastic dynamic systems. First, the extended Kalman filter is used to estimate the unknown states online, and the estimation of posterior states are used as the input of the neural network compensator, so that the unknown states which are difficult to use in basic NMPC can be fully applied in the compensation control input; Then, the kernel density estimation is used to indirectly obtain the control error entropy of the non-Gaussian dynamic system. Guided by the optimization performance index which is constructed mainly about the control error entropy, the output weight of the compensator is optimized to tune the compensation effect; Finally, compensation control and basic predictive control are integrated to achieve high-performance control of stochastic dynamic systems. The control error of the proposed method and the upper bound of the state estimation error are analyzed by inductive reasoning method to ensure that the closed-loop system has input-to-state stability about the disturbances. Data experiments of sewage treatment process verify the superiority and practicability of the proposed method.

Index Terms—Nonlinear model predictive control (NMPC), enhanced NMPC(En-NMPC), compensation control, entropy optimization, unknown state estimation, input-to-state stability, wastewater treatment process (WWTP)

I. INTRODUCTION

AS a primary multivariable control method in industrial practice, model predictive control (MPC) successfully obtains the optimal control law in the prediction horizon by solving an optimal control problem (OCP), and further extends the feedback stabilization which is common in conventional control methods to global optimization [1]-[3]. With the massive increase in computer performance, the problem of practical application of model predictive control caused by computing pressure has been greatly alleviated, so the research on the new framework of model predictive

control with high performance has received extensive attention from both industry and academia [3], [4]. From the perspective of the system, the existing MPC research is mainly divided into two types, namely MPC for deterministic system and MPC for uncertainty system. MPC for deterministic system (also known as deterministic MPC) has mature solutions from 2000, but for uncertain system, whether in the form of additive disturbances, state error, or model error, uncertain MPC is still a research topic in the current academic circles.

For the uncertain MPC problem, it is usually not the best optimal control law by solving the open-loop optimal control problem without considering the uncertainties in the prediction horizon [5]-[7]. At present, uncertainty MPC is mainly divided into two categories, namely robust MPC (RMPC) [6] and stochastic MPC (SMPC) [7]. Liu et al. [8] proposed a robust min-max RMPC algorithm, which tries to find the optimal control law in the worst case caused by uncertainties to ensure stability, so the performance of the control law obtained by the algorithm is relatively conservative. In order to further reduce the conservation of the algorithm, a Tube-based RMPC algorithm is proposed in [9], which separates the deterministic system from the actual system by adopting the separation control strategy. Then, by transforming the control of the actual system into the control of the deterministic system and restricting the system states in a subset of constraints, this method effectively reduces the conservatism. In general, the RMPC algorithm can only handle the problems under the bounded and determined uncertainties. To deal with the control problems with more constraints of uncertainties, the SMPC based on scenario generation is proposed in [10]. This method uses the probability density function (PDF) of disturbances to sample a large number of independent and identically distributed disturbances. Due to the solution of the OCP based on scenario generation will tend to the solution of the original OCP with a high probability, the control algorithm can deal with more various constraint types of noises, when the number of scenarios reaches a certain amount.

It should be pointed out that the deterministic MPC usually does not consider the influence of uncertain factors when designing the control law. It only calculates the predictive control law by a nominal model, and then analyzes the performance of the closed-loop control system for a certain uncertainty under the control algorithm, so the algorithm itself lacks a dynamic rejection mechanism for random disturbances [11]; While the uncertainty MPC considers the influence of uncertain factors during the design of the controller, it turns the optimization problem into a minimum-maximization problem to get a conservative solution.
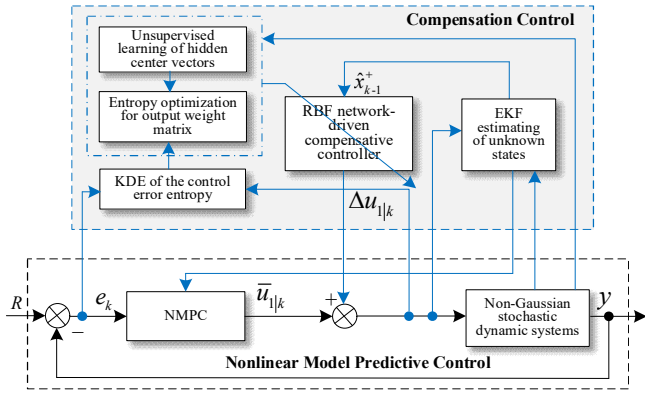
Fig.1. The control architecture of the proposed En-NMPC

Therefore, the assumptions required to ensure the stability of the algorithm are generally more conservative, and the control effects are affected by the types of noises. Sometimes it is hard to obtain a feasible solution when the conditions are extreme [7]. Moreover, some deterministic MPC algorithms have been applied to a certain extent in practice due to their simple forms and better decoupling control effects especially when the operating conditions are stable and less noisy. Such as the work in [12] achieves good decoupling effects in the polymerization reactor by using the deterministic MPC algorithm. However, when the operating conditions and disturbances change greatly, these methods always tend to poor control effects, due to the lack of a mechanism to dynamically adjust for such disturbances and other stochastic uncertainties. When facing the impact of strong noises and disturbances, then, if turning to adopt the uncertain MPC algorithm, such as the above RMPC or SMPC, the existing predictive control structure can only be abandoned and the control structure should be redesigned according the uncertain MPC algorithm at a great cost. On the contrary, the control effect of uncertain MPC will become more conservative, when the conditions gradually tend to stable again. Therefore, in view of the stochastic noises and strong disturbances which are common in practical industry systems, how to improve the performance of existing deterministic MPC at low cost without changing the existing predictive control structures is the focus of this paper.

Focus on the above challenges, this paper proposes a novel enhanced NMPC (En-NMPC) method based on online estimation of unknown states and neural network dynamic compensation of control error with entropy optimization. As shown in Fig.1, the proposed En-NMPC is mainly divided into two parts, namely the deterministic NMPC part and the proposed compensation control part. The main innovations of the proposed method are as follows:

1) In order to make full use of the unknown state information of the stochastic dynamic system during control [13],[14], the extended Kalman filter (EKF) is used to estimate the unknown or unmeasurable states online, so that the estimated posteriori state information can be fully applied in the compensation control part.

2) The RBF network [15]-[17] is used to nonlinearly map the posteriori states of the dynamic system, estimated by the EKF, to obtain the optimal compensation for the control input calculated by the deterministic NMPC. By tunning the output weight of the RBF compensator based on minimizing the performance index about the control error entropy indirectly calculated by kernel density estimation [15], [16], it can effectively reduce the

fluctuation of control error caused by non-Gaussian noises and stochastic disturbances. Moreover, the Elbow algorithm [18] and the K-means clustering algorithm are used to obtain the center vectors of the hidden layers.

3) The inductive reasoning method is used to prove that the controlled system has input-to-state stability (ISS) under the disturbances, and the state estimation calculated by EKF has bounded-error, which ensure the stability and excellent control performance of the proposed control strategy. At the same time, the effectiveness and superiority of the proposed method are verified through data experiments of sewage treatment process.

Notation: *Define the upper bound of x is $|x| =$ $\sup\{\|x_k\|, k \in \mathbb{Z}_+\}$; Continuous function $h_1 : \mathbb{R}^+ \to \mathbb{R}^+$ is a class K function which means it is monotonically decreasing and satisfies $h_1(0) = 0$; $h_2 : \mathbb{R}^+ \to \mathbb{R}^+$ is a class K_∞ function which means that it is a K function and satisfies $h_2(s) \to \infty, s \to \infty$; $h_3 : \mathbb{R}^+ \times \mathbb{R}^+ \to \mathbb{R}^+$ is a class KL function, for any $t \ge 0$, $h_3(\cdot, t)$ is K function, and $h_3(s, \cdot)$ is monotonically decreasing with $h_3(s, t) \to 0, t \to \infty$ for any $s>0$.*

II. PROBLEM STATEMENT

Consider the following nonlinear dynamic system:

$$x_{k+1} = f(x_k, u_k, w_k) \tag{1}$$
$$y_k = h(x_k, u_k, v_k) \tag{2}$$

where $x_k \in \mathbb{R}^n$ represents the state, and $y_k \in \mathbb{R}^m$ indicates the measured output, and $u_k \in \mathbb{R}^n$ is the control input. w_k means the additive process noise, and v_k is the additive measurement noise. $f(\cdot)$ and $h(\cdot)$ are the nonlinear equations.

For the dynamic nonlinear discrete-time system described in Eqs.(1) and (2), its nominal model is:

$$x_{k+1} = f_{nom}(x_k, u_k) \triangleq f(x_k, u_k, 0) \tag{3}$$
$$y_k = h_{nom}(x_k, u_k) \triangleq h(x_k, u_k, 0) \tag{4}$$

where $f_{nom}(.)$ and $h_{nom}(.)$ are the nonlinear functions of the nominal model of the system without considering the influence of noises. For the deterministic NMPC shown in Fig.1, the optimal control problem in the finite time horizon of the discrete-time system based on Eqs.(3) and (4) is expressed as the following Problem 1:

Problem 1: *Let x_k is the discrete-time system state at sample time k, and the optimization problem of the nonlinear predictive control under the quasi-infinite time horizon can be described as:*

$$\min_{\bar{u}} J(x_0, u(\cdot)) = \sum_{i=0}^{N-1} F(\bar{x}_{k+i|k}, \bar{u}_{k+i|k}) \tag{5}$$

The following constraints are satisfied during prediction horizon:

$$\begin{cases} \bar{x}_{i+1|k} = f_{nom}(\bar{x}_{i|k}, \bar{u}_{i|k}), \bar{x}_{k|k} = x_k \\ \bar{u}_{i|k} \in U, \ i \in [k, k+N-1] \\ \bar{x}_{i|k} \in X, \ i \in [k, k+N-1] \end{cases} \tag{6}$$

Even without un-modeled error and external disturbances, the system states obtained in the prediction horizon may also be different from the actual system due to the finite horizon. Therefore, in order to better distinguish the states in the prediction horizon from the real states. We use $\bar{x}_{i|k}$ to represent the state and $\bar{u}_{i|k}$ represent the control input in prediction horizon. Besides, X and U are respectively the

constraint domain of the state and control input. To simplify the analysis, the prediction horizon and the control horizon are the same. In Eq.(5), $F(x,u): X \times U \to \mathbb{R}$ is continuous with respect to the variables x and u, and simultaneously satisfies $F(\mathbf{0},\mathbf{0}) = 0$, and also satisfies with $F(x,u) > 0$, $(x,u) \in X \times U \setminus \{\mathbf{0},\mathbf{0}\}$.

For Problem 1, there are many classical results, such as the algorithm in [11]. However, they do not consider the influence of disturbances on the system. Actually, the practical industrial systems are widely affected by various noises and uncertain dynamics, thus [11] is not the optimal solution of the Problem 1. To fix this, this paper designs the compensation control input $\Delta U_k = [\Delta u_{1|k}, \Delta u_{2|k}, \cdots, \Delta u_{N|k}]^{\mathrm{T}}$, then makes $U_k^* = U_k + \Delta U_k$ tend to the optimal solution as much as possible. Since NMPC solves a new optimal control problem at every sample time, and only applies the first element of the control sequence to the actual controlled plant, it only needs to design $\Delta u_{1|k}$ so that:

$$u_{1|k}^* \approx \bar{u}_{1|k} + \Delta u_{1|k} \tag{7}$$

For the proposed En-NMPC, the basic predictive control input and the compensation control input are respectively obtained by:

$$\bar{u}_{1|k} = \arg\min_{\bar{u}} J(x_0, u(\cdot)) = \sum_{i=0}^{N-1} F(\bar{x}_{k+i|k}, \bar{u}_{k+i|k}) \tag{8}$$

$$\Delta u_{1|k} = W_k^{\mathrm{T}} \Phi(\hat{x}_k^+) \tag{9}$$

where $\bar{u}_{1|k}$ is the basic prediction control input by solving Problem 1, and $\Delta u_{1|k}$ is the compensation control input by the proposed compensator; $\Phi(\cdot) \in \mathbb{R}^p$ is the RBF of the compensator, $\hat{x}_k^+$ is the estimated value of the unknown state obtained by EKF, and W_k^{T} is the output weight matrix of RBF network compensator. Moreover, x_0 is the initial state, $u = \{u_0, u_1, \cdots\}$ is the control sequence.

Remark 1: *For the proposed En-NMPC, $\Delta u_{1|k}$ can be obtained by tuning W_k^{T} of the RBF network compensator in Eq.(9). This adjustment can be achieved through online or offline data learning according to the operating conditions, which will be described in detail in Section III below. To facilitate the subsequent analysis, the state $x_k = \varphi(k; x_0, w)$ of the system at time k is represented by the function $\varphi(\cdot)$ which can be derived recursively by Eqs.(1) and (2), and the same as the following generalized system depicted by Eq.(39). Here, $w = \{w_0, w_1, \cdots\}$ is the disturbance sequence.* □

III. CONTROL ALGORITHM

This section presents the specific algorithm of the En-NMPC shown in Fig.1, which mainly includes two parts: the unknown state estimation by EKF and the RBF network compensator with entropy optimization. Since the basic deterministic NMPC mainly solves Eq.(8), it has been discussed in many literatures, such as in [5],[11], so it will not be repeated here.

A. Unknown State Estimation by EKF

For multivariable stochastic dynamic systems, in order to make full use of the unknown internal state information during control, the EKF technique is used to estimate the unmeasurable or unknown internal states online [19]. The EKF online estimation algorithm is mainly composed of two parts: state prediction and state updating.

The state prediction algorithm is as follows:

$$P_k^- = A_{k-1} P_{k-1}^+ A_{k-1}^{\mathrm{T}} + F_{k-1} Q_{k-1} F_{k-1}^{\mathrm{T}} \tag{10}$$

$$\hat{x}_k^- = f(\hat{x}_{k-1}^+, u_{k-1}) \tag{11}$$

where $A_{k-1} = \partial f / \partial x|_{\hat{x}_{k-1}^+}$ and $F_{k-1} = \partial f / \partial w|_{\hat{x}_{k-1}^+}$.

The state updating algorithm is as follows:

$$K_k = P_k^- C_k^{\mathrm{T}} (C_k P_k^- C_k^{\mathrm{T}} + Z_k G_k Z_k^{\mathrm{T}})^{-1} \tag{12}$$

$$\hat{x}_k^+ = \hat{x}_k^- + K_k (y_k - h(\hat{x}_k^-, u_k)) \tag{13}$$

$$P_k^+ = (I - K_k C_k) P_k^- \tag{14}$$

where $C_k = \partial h / \partial x|_{\hat{x}_k^-}$ and $Z_k = \partial h / \partial v|_{\hat{x}_k^-}$.

In Eqs.(10)-(14), $\hat{x}_k^-$ stands for the priori estimated state, $\hat{x}_k^+$ is the posterior estimated state, K_k is the Kalman gain matrix updated by Eq.(12) at each sample moment, P_k^- represents the transfer matrix of priori estimation, and P_k^+ stands for the transfer matrix of posterior estimation. Moreover, G_k is the variance of the measured noise and Q_k is the variance of process noise.

Assumption 1: *In Eqs.(1) and (2), $w_k, v_k \in \Omega$ are two bounded, zero-means, non-Gaussian and mutually independent noises, and Ω is the constraint domain of the noises. Their respective variances can be calculated, but the probability density functions (PDF) are unknown.* □

Remark 2: *Since using the EKF to estimate the states, it is necessary to ensure Assumption 1 that the variance of w_k and v_k can be calculated or already known. However, if the system states do not need to be estimated by EKF, the prior information about respective variance of w_k and v_k is not required. As for the other part of the proposed algorithm, it has no special restriction on the respective PDF of w_k and v_k, so long as the noise are bounded and mutually independent.* □

B. Learning Based Control Error Compensation

In this paper, a three-layer RBF network is selected to construct the compensation controller for the proposed En-NMPC to obtain the optimal compensation control input. The input of the RBF network compensator is the state $\hat{x}_k^+$ estimated by the EKF, and the output of the hidden layer is $\Phi(\hat{x}_k^+)$ which is depicted by Eq.(15), and $\Delta u_{1|k}$ is the output of the compensator calculated by Eq.(16):

$$\begin{cases} \Phi(\hat{x}_k^+) = [\phi_1(\hat{x}_k^+), \phi_2(\hat{x}_k^+), \cdots, \phi_p(\hat{x}_k^+)] \\ \phi_i(\hat{x}_k^+) = \exp\left(-\left\|\hat{x}_k^+ - c_i\right\|^2 / \sigma_{\mathrm{rbf}}^2\right), i = 1, 2, \cdots, p \end{cases} \tag{15}$$

$$\begin{cases} \Delta u_{1|k} = W_k^{\mathrm{T}} \Phi(\hat{x}_k^+) \\ W_k = [w_1, \cdots, w_l, \cdots, w_p]^{\mathrm{T}} \end{cases} \tag{16}$$

where c_i is the center vectors of G_i, and G_i is the category divided from $\hat{X} = \{\hat{x}_1^+, \cdots, \hat{x}_i^+, \cdots, \hat{x}_k^+\}$ by the partition function $C(i)$, whose definition is given in the following section. Moreover, p is the given number of the center vectors, σ_{rbf} is the width of the kernel, and W_k is the output weight matrix of the compensator.

1) Unsupervised Learning of Hidden Center Vectors

At the stage of unsupervised learning of hidden center vectors, the Elbow algorithm in [18] is first used to obtain the number p of cluster centers. Then, the unsupervised K-means clustering algorithm is used to calculate the cluster centers of the given input data set $\hat{X} = \{\hat{x}_1^+, \cdots, \hat{x}_i^+, \cdots, \hat{x}_k^+\}$ which are used as the center vectors of the hidden layer. Specifically, the data set $\hat{X}$ is divided into p classes G_i, and the classes are satisfied with:

$$G_i \bigcap G_j = \varnothing \text{ and } \bigcup_{i=1}^p G_i = X$$

The cluster centers of G_i is c_i, then $c = [c_1, \cdots, c_p]$ is used as the center vectors of the hidden layer. At the same time, each

Algorithm 1: Unsupervised learning of c_i in RBF network compensator
Input: The data set $\hat{X} = \{\hat{x}_1^+, \cdots, \hat{x}_i^+, \cdots, \hat{x}_k^+\}$.
Output: The number p of center vectors and the center vectors.
1: Calculate p by using the Elbow algorithm in [18].
2: Randomly select p samples as the initial cluster centers c^t at $t=0$:
3: Cluster the samples by $\arg\min_{C^t} \sum_{l=1}^{p} \sum_{C^t(i)=l} \| \hat{x}_i - c_l^t \|^2$, where $C^t(i)=l$ is the partition function at t time.
4: Assign each sample to the class of its nearest center.
5: Calculate $c_l^{t+1} = \sum_{C^t(i)=l} \hat{x}_i^+ / n_l$ as the new cluster centers.
6: If the iterations converge, stop training, else $t=t+1$ and turn to Step 2.

x_i of the k samples in $\hat{X}$ are respectively represented by an integer $i = \{1, 2, \cdots, k\}$, and each G_l of the p classes is represented by an integer $l = \{1, 2, \cdots, p\}$. Then, the partition function $C(i)=l$ is used to represent the mapping of the sample x_i to G_l. The detailed solving algorithm is shown in Algorithm 1.

2) Entropy Optimization Based Supervised Learning for Weight Matrix

After the center vectors of the hidden layer are determined, the gradient descent algorithm is used to further tune the output weight matrix W_k of the network. Since it is a kind of supervised learning, it is necessary to first design a suitable optimization performance index. Conventional performance indicators such as mean and variance cannot fully describe the characteristics of non-Gaussian dynamic systems, so entropy indicator is used to help construct the performance index. Compared to the indicators of mean and variance, entropy is a more effective measure of the diversity, uncertainty and randomness of data [19], [20]. The smaller the entropy is, the less volatility and randomness of that data are. Specific to the control error, the smaller the control error entropy is, the higher the stability of the closed-loop system and the smaller the control error fluctuation are.

The entropy $H_2(q_l)$ of random variable q_l is calculated by:

$$H_2(q_l) = -\log V(q_l) \tag{17}$$

where $V(q_l)$ is the information potential of q_l. The entropy $H_2(q_l)$ is decreasing with respect to $V(q_l)$. In order to reduce the computation cost, the optimization of the entropy of the control error can be transferred to optimize the information potential. However, the entropy of a set of data can only reflect the fluctuation, so it is necessary to add a limit to the mean of control error in the performance index to achieve stable tracking control.

To sum up, for the multivariable stochastic dynamic system, the following performance index about the entropy of the control error is defined as follows:

$$J_k = -R_1 \sum_{i=1}^{m} V(e_i^k) - R_2 V_{\text{joint}}(e_k) \\ + R_3 \sum_{i=1}^{m} E(e_i^k) + R_4 \Delta u_{1|k}^{\text{T}} \Delta u_{1|k} \tag{18}$$

where m is the number of output, $\Delta u_{1|k}^{\text{T}} \Delta u_{1|k}$ represents the energy of compensation input, R_1, R_2, R_3, R_4 are given constants, $e_{i,k}$ is the control error of the i-th output at k time. To further analysis, $e_i^k = [e_{i,1}, \cdots, e_{i,k}]$ is the control error of the i-th output from beginning to k time, and $e_k = [e_1^k, \cdots, e_m^k]$ are the control error of m outputs. Moreover, $V_{\text{joint}}(e_k)$ is the joint information potential of data e_k, and $E(e_i^k)$ is the mean value of the control error which can be calculated by:

$$E(e) = \int e \hat{\gamma}_e(e) de \tag{19}$$

and it is used to characterize the magnitude of the control error.

In Eq.(18), the edge information potential $V(q_l)$ and the joint information potential $V_{\text{joint}}(Q)$ can be calculated as follows:

$$\begin{cases} V(q_l) = \int \gamma_{q_l}^2(q_l) \mathrm{d}q_l \\ V_{\text{joint}}(Q) = \int \cdots \int \left(\gamma_Q(q_1, \cdots, q_m) \right)^2 \mathrm{d}q_1 \cdots q_m \end{cases} \tag{20}$$

where $Q = [q_1, \cdots, q_l, \cdots, q_m]$ are m random variables, γ_{q_l} is the PDF of variable q_l, γ_Q is the joint PDF of Q.

Due to the precise statistical PDF of control error is not available for practical industrial processes in advance, the kernel density estimation (KDE) [15], [20] is used to calculate the PDF of the control error. Aim to the PDF of q_l and the joint PDF of Q, they are usually calculated by the following equations:

$$\begin{cases} \hat{\gamma}_{q_l}(q_l) = N^{-1} \sum_{i=1}^{N} \kappa_{\sigma_l}(q_l - q_{l,i}) \\ \kappa_{\sigma_l}(q_l) = (\sqrt{2\pi}\sigma_l)^{-1} \exp(-q_l^2 / 2\sigma_l^2) \end{cases} \tag{21}$$

$$\begin{cases} \hat{\gamma}_Q(q_1, \cdots, q_m) = N^{-1} \sum_{i=1}^{N} \kappa_\Sigma(q_1 - q_{1,i}, \cdots, q_m - q_{m,i}) \\ \kappa_\Sigma(q_1, \cdots, q_m) = \prod_{l=1}^{m} \kappa_{\sigma_l}(q_l) \end{cases} \tag{22}$$

where $\kappa_{\sigma_l}(q_l)$ is the Gaussian kernel function for each variable q_l, and $\{q_{l,1}, \cdots, q_{l,N}\}$ are the N independent identically distributed samples of variable q_l. Here, Eq.(21) is used to calculate the PDF for one dimensional data, while Eq.(22) is used to calculate the joint PDF for multi-dimensional data.

It can verify that the Gaussian kernel function satisfies:

$$\lim_{q_l \to \infty} | q_l \kappa_{\sigma_l}(q_l) | = 0, \ \kappa_{\sigma_l}(q_l) \geq 0, \ \int \kappa(q_l) \mathrm{d}q_l = 1 \tag{23}$$

That is it meets the validity requirement of KDE on kernel function.

Noted that the integration of the product of two Gaussian function can still be evaluated by another Gaussian function. For ease of calculation, by putting Eq.(21) into Eq.(20), the calculation of the edge information potential $V(q_l)$ can be transferred into the following way:

$$\begin{aligned} V(q_l) &= \int (N^{-1} \sum_{i=1}^{N} \kappa_{\sigma_l}(q_l - q_{l,i}))^2 \mathrm{d}q_l \\ &= N^{-2} \int (\sum_{i=1}^{N} \sum_{j=1}^{N} \kappa_{\sigma_l}(q_l - q_{l,i}) \kappa_{\sigma_l}(q_l - q_{l,j})) \mathrm{d}q_l \\ &= N^{-2} \sum_{i=1}^{N} \sum_{j=1}^{N} \int \kappa_{\sigma_l}(q_l - q_{l,i}) \kappa_{\sigma_l}(q_l - q_{l,j}) \mathrm{d}q_l \\ &= N^{-2} \sum_{i=1}^{N} \sum_{j=1}^{N} \kappa_{\sigma_l \sqrt{2}}(q_{l,j} - q_{l,i}) \end{aligned}$$

Similar to this, by putting Eq.(22) into Eq.(20), the calculation of joint information potential $V_{\text{joint}}(Q)$ is transferred into the following condensed form to calculate:

$$\begin{aligned} V_{\text{joint}}(Q) &= \int \cdots \int \left(\gamma_Q(q_1, \cdots, q_m) \right)^2 \mathrm{d}q_1 \cdots q_m \\ &= \int \cdots \int (\frac{1}{N} \sum_{i=1}^{N} \kappa_\Sigma(q_1 - q_{1,i}, \cdots, q_m - q_{m,i}))^2 \mathrm{d}q_1 \cdots q_m \\ &= N^{-2} \int \cdots \int (\sum_{i=1}^{N} \sum_{j=1}^{N} \kappa_\Sigma(q_1 - q_{1,i}, \cdots, q_m - q_{m,i}) \\ &\qquad \times \kappa_\Sigma(q_1 - q_{1,j}, \cdots, q_m - q_{m,j})) \mathrm{d}q_1 \cdots q_m \\ &= N^{-2} \sum_{i=1}^{N} \sum_{j=1}^{N} \int \cdots \int (\kappa_\Sigma(q_1 - q_{1,i}, \cdots, q_m - q_{m,i}) \\ &\qquad \times \kappa_\Sigma(q_1 - q_{1,j}, \cdots, q_m - q_{m,j})) \mathrm{d}q_1 \cdots q_m \\ &= N^{-2} \sum_{i=1}^{N} \sum_{j=1}^{N} \int \cdots \int [\prod_{l=1}^{m} \kappa_{\sigma_l}(q_l - q_{l,j}) \\ &\qquad \times \prod_{l=1}^{m} \kappa_{\sigma_l}(q_l - q_{l,i})] \mathrm{d}q_1 \cdots q_m \end{aligned}$$

Input: The estimation of state $\hat{x}_k^+$.

Output: The weight W_k of output layer.

1: Initialize W_k, the learning rate η, and the threshold $\tilde{\varepsilon}$.

2: Obtain the gradient of Eq.(18) as $\nabla J_k = \partial J_k/\partial W_{k-1}|\ W_{k-1}$.

3: If $\nabla J_k \nabla J_k^T < \tilde{\varepsilon}$, and then the best weight is W_{k-1}, else return to Step 4.

4: Update the weight by $W_k = W_{k-1} - \eta \nabla J_k$.

5: Return to Step 2.

Algorithm 3: En-NMPC implementation algorithm

1: Find the center vectors of the RBF compensator by Algorithm 1.

2: Estimate the information potential of control error by Eqs.(20)-(22).

3: Calculate the optimization performance index by Eq.(18).

4: Estimate $\hat{x}_k^+$ by Eqs. (10)-(14).

5: Obtain the optimal W_k by Algorithm 2.

6: Calculate $\bar{u}_{1|k}$ by Eq. (8) and calculate $\Delta u_{1|k}$ by Eq.(9).

7: Calculate $u_{1|k}^*$ by Eq.(7).

8: Apply $u_{1|k}^*$ to the system, and put $k = k+1$, then return to Step 5.

$$
\begin{aligned}
&= N^{-2} \sum_{i=1}^{N} \sum_{j=1}^{N} [\int \kappa_{\sigma_1}(q_1 - q_{1,i})\kappa_{\sigma_1}(q_1 - q_{1,j})\mathrm{d}q_1 \\
&\quad \cdots \int \kappa_{\sigma_m}(q_m - q_{m,i})\kappa_{\sigma_m}(q_m - q_{m,j})\mathrm{d}q_m] \\
&= N^{-2} \sum_{i=1}^{N} \sum_{j=1}^{N} \prod_{l=1}^{m} \kappa_{\sigma_l \sqrt{2}}(q_{l,j} - q_{l,i})
\end{aligned}
$$

Thus, in order to facilitate the calculation in the computer, Eq.(20) is transferred into the following easy form to calculate:

$$
\begin{cases}
V(q_l) = \int \gamma_{q_l}^2 (q_l)\mathrm{d}q_l \\
\quad = N^{-2} \sum_{i=1}^{N} \sum_{j=1}^{N} \kappa_{\sigma_l \sqrt{2}}(q_{l,j} - q_{l,i}) \\
V_{\text{joint}}(Q) = \int \cdots \int (\gamma_Q (q_1, \cdots, q_m))^2 \mathrm{d}q_1 \cdots q_m \\
\quad = N^{-2} \sum_{i=1}^{N} \sum_{j=1}^{N} \prod_{l=1}^{m} \kappa_{\sigma_l \sqrt{2}}(q_{l,j} - q_{l,i})
\end{cases} \tag{24}
$$

After determining the performance index described in Eq.(18), the output weight matrix W_k of the compensator is optimized by the gradient descent algorithm. The RBF neural network has a unique and determined optimal solution and does not exist local minimum problem such as the BP neural network, this is mainly because the final output is only a linear combination between the hidden layer and W_k. The implementation steps of the output weight optimization by gradient descent algorithm are shown in Algorithm 2.

3) Implementation Steps of the En-NMPC

After obtaining the optimal W_k, the final output of the RBF network compensator can be calculated by Eq.(9), which will be used as the compensation control input to the basic NMPC. Then the final integrated control input is applied to the controlled dynamic system to enhance the control performance. In summary, the specific steps of the proposed En-NMPC method are given in Algorithm 3.

Remark 3: *The stable output of the RBF network compensator is the prerequisite for the efficient operation of the proposed control algorithm, so the effective learning of the RBF network is extremely important. When the controlled plant facing with a poor environment, the online learning can be used to adjust the weights of the output layer in real time, so as to ensure the performance of the compensation. At the same time, due to the simple structure of the RBF network, the online learning time generally meets the sampling interval requirements. When the environment improves, in order to avoid the computational pressure of online learning, the historical data can be used for offline learning by Steps*

1-5 in Algorithm 3. When the output weights of the compensator tend to converge, the obtained compensator is directly applied to the actual system by Steps 6-8 to improve the control performance. □

Remark 4: *To analyze the convergence of W_k, the second derivative of the function Eq.(18) is defined as $R = \nabla^2 J_k$. Then, Algorithm 2 can ensure the mean square convergence of W_k, when the learning rate η satisfies $0 < \eta < 2/\max\{\lambda_i\}$, where $\lambda_i, i = 1, \cdots, l$ are the eigenvalues of R. Therefore, the convergence can be further guaranteed by tuning R_1, R_2, R_3, R_4 in Eq.(18) which are directly relevant to $R = \nabla^2 J_k$.* □

IV. PERFORMANCE ANALYSIS

For the proposed En-NMPC, the mechanism of control is to add the compensation control input to the basic predictive control input. Therefore, the stability of the proposed En-NMPC algorithm is proved by recursively analyzing the norm of the input and output after adding the compensation. For the nonlinear system shown in Eqs.(1) and (2), in order to facilitate the stability analysis of the control algorithm, the following assumptions are made at first.

Assumption 2: *The nonlinear dynamic system shown in Eqs.(1) and (2) can be approximated by the following equations:*

$$
x_k \approx A x_{k-1} + B u_{k-1} + F w_{k-1} + \Delta f_{k-1}(x_{k-1}, u_{k-1}, w_{k-1}) \tag{25}
$$

$$
y_k \approx C x_k + D u_k + Z v_k + \Delta h_k(x_k, u_k, v_k) \tag{26}
$$

where A,B,C,D,F and Z are the system matrices of appropriate dimension obtained by linearizing the nonlinear system, $\triangle f_{k-1}$ and $\triangle h_k$ are the remaining unmodeled dynamic terms after linearizing the nonlinear system. □

Remark 5: *The linear model, obtained by linearizing the nonlinear dynamic system at the operating point, can usually still guarantee the qualitative prediction of the dynamic behavior of the system. Actually, it is a common approach to use the above linearized model to analyze the stability [21].* □

Assumption 3: *Aim to the remaining unmodeled dynamic terms $\triangle f_{k-1}$ and $\triangle h_k$ depicted by Eqs.(25) and (26), there exists the constants $L_1 \sim L_5$ that satisfy the following equations:*

$$
\|\Delta f_{k-1}\| \le L_1 \|x_{k-1}\| + L_2 \|u_{k-1}\| + L_3 \|w_{k-1}\| \tag{27}
$$

$$
\|\Delta h_k\| \le L_4 \|x_k\| + L_5 \|u_k\| + L_6 \|v_k\| \tag{28}
$$

Remark 6: *Considering $\triangle f_{k-1}$ and $\triangle h_k$ are the remaining unmodeled dynamic terms after linearizing at operating points, the norms of $\triangle f_{k-1}$ and $\triangle h_k$ are usually bounded within a range, so the Assumption 3 is always hold, because the real positive numbers $L_1 \sim L_5$ can be adjusted by the norms of x_k, u_k, w_k and v_k.* □

Assumption 4: *Aim to the dynamic system shown in Eq.(1), $f(.)$ satisfies the following Lipschitz condition:*

$$
\|f(x_1, u_{k-1}, w_{k-1}) - f(x_2, u_{k-1}, 0)\| \le L \|x_1 - x_2\| \tag{29}
$$

where L is the Lipschitz constant. □

Assumption 5: *For the unmodeled dynamic term $\triangle h_k$ in Eq.(26) and the unmodeled dynamic term $\triangle h_{2k}$ for EKF, there is a constant L_7 which ensures the following equation hold:*

$$
\|\Delta h_k - \Delta h_{2k}\| \le L_7 \|x_k - \hat{x}_k^+\| \tag{30}
$$

where $\hat{x}_k^+$ is the estimation of state. □

Lemma 1: *The norm of the final integrated control input of En- NMPC shown in Eqs.(7)-(9) is bounded:*

$$\|u_k\| \le \|\bar{u}_{1|k}\| + \|\Delta u_{1|k}\| = \|\bar{u}_{1|k}\| + \|W_k^{\mathrm{T}}\Phi(\hat{x}_k^+)\| \le \nu(W) \quad (31)$$

Proof: In Eqs.(7)-(9), $\bar{u}_{1|k}$ is the input obtained by the basic NMPC. Since the control input has been restricted during the rolling optimization, $\bar{u}_{1|k}$ is bounded. Considering that the hidden layer of the RBF network compensator is a Gaussian kernel function and the output layer is only a linear combination between weight matrix and hidden layer, the compensation control input $\Delta u_{1|k}$ is also bounded, that is, the final control input u_k is bounded and Eq.(31) holds.

Lemma 2: *Under Assumption 3, in order to facilitate the analysis of the system stability, redefine the vector $\varepsilon_k=[x_k,z_k]$, where x_k is the control error, and z_k is the cumulative control error, then on the basis of Eq.(27), there exists the following inequality:*

$$\|\Delta f_k\| \le L_1\|\varepsilon_k\| + L_2\|u_k\| + L_3\|w_k\| \quad (32)$$

Proof: It is easy to find that $\|x_k\| \le \|\varepsilon_k\|$ from $\varepsilon_k = [x_k, z_k]$, then by putting it into Eq.(27), we can obtain:

$$\begin{aligned}\|\Delta f_k\| &\le L_1\|x_k\| + L_2\|u_k\| + L_3\|w_k\| \\ &\le L_1\|\varepsilon_k\| + L_2\|u_k\| + L_3\|w_k\|\end{aligned} \quad (33)$$

Lemma 3: *On the basis of Assumptions 2 and 3, there always exists constants M_1, M_2, M_3 that satisfy the following inequalities:*

$$\|\Delta h_k\| \le M_1\|\varepsilon_{k-1}\| + M_2\nu(W) + M_3\|w_{k-1}\| + L_6\|v_k\| \quad (34)$$

where $M_1 = L_4\|A\| + L_4L_1, M_2 = L_4\|B\| + L_4L_2 + L_5$ and $M_3 = L_4\|F\| + L_4L_3$. □

Proof: On the basis of Assumption 4, by substituting Eq.(25) into Eq.(28), it can be known that:

$$\begin{aligned}\|\Delta h_k\| &\le L_4\|x_k\| + L_5\|u_k\| + L_6\|v_k\| \\ &\le L_4\|Ax_{k-1} + Bu_{k-1} + Fw_{k-1} + \Delta f_{k-1}\| + L_5\|u_k\| + L_6\|v_k\| \\ &\le L_4\|A\|\|x_{k-1}\| + L_4\|B\|\|u_{k-1}\| + L_4\|F\|\|w_{k-1}\| \\ &\quad + L_4\|\Delta f_{k-1}\| + L_5\|u_k\| + L_6\|v_k\|\end{aligned} \quad (35)$$

Substituting Eq.(32) into Eq.(35), it can obtain:

$$\begin{aligned}\|\Delta h_k\| &\le L_4\|A\|\|\varepsilon_{k-1}\| + L_4\|B\|\|u_{k-1}\| + L_4\|F\|\|w_{k-1}\| \\ &\quad + L_4(L_1\|\varepsilon_{k-1}\| + L_2\|u_{k-1}\| + L_3\|w_{k-1}\|) + L_5\|u_k\| + L_6\|v_k\| \\ &\le (L_4\|A\| + L_4L_1)\|\varepsilon_{k-1}\| + (L_4\|B\| + L_4L_2)\|u_{k-1}\| \\ &\quad + L_5\|u_k\| + (L_4\|F\| + L_4L_3)\|w_{k-1}\| + L_6\|v_k\| \\ &\le M_1\|\varepsilon_{k-1}\| + M_2\nu(W) + M_3\|w_{k-1}\| + L_6\|v_k\|\end{aligned} \quad (36)$$

A. Input to State Stability (ISS)

In order to analyze the input to state stability of the proposed En-NMPC, on the basis of the above Assumptions 2-5 and Lemmas 1 and 2, the recurrence relation of the control error is shown in the following:

$$x_k \approx Ax_{k-1} + Bu_{k-1} + Fw_{k-1} + \Delta f_{k-1} \quad (37)$$

The cumulation of the control error z_k is shown as follows:

$$\begin{aligned}z_k &\approx z_{k-1} + e_k = z_{k-1} + r - y_k \\ &\approx z_{k-1} + r - CAx_{k-1} - CBu_{k-1} \\ &\quad - CFw_{k-1} - C\Delta f_{k-1} - Du_k - Zv_k - \Delta h_k\end{aligned} \quad (38)$$

Therefore, taking Eqs.(37) and (38) into $\varepsilon_k=[x_k, z_k]$, it can be further converted to the following generalized system:
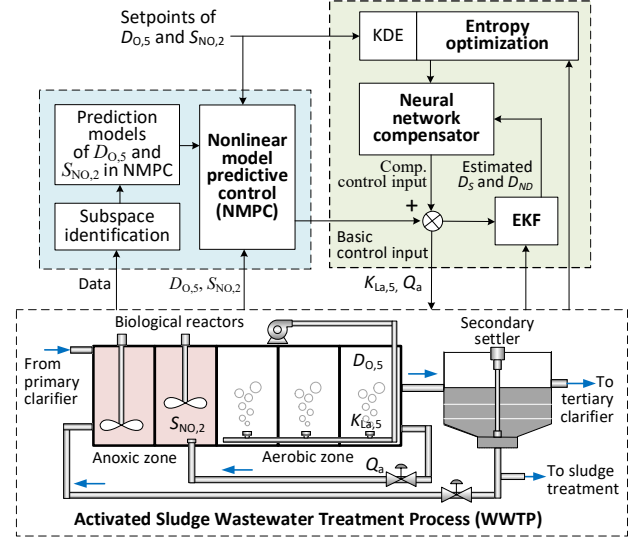

Fig.2 Control of WWTP with the proposed En-NMPC

$$\begin{aligned}\varepsilon_k &= \bar{A}\varepsilon_{k-1} + \bar{B}_1 u_{k-1} + \bar{B}_2 u_k + \bar{F}_1 w_{k-1} \\ &\quad + \bar{F}_2\Delta f_{k-1} + \bar{Z}v_k + \bar{H}\Delta h_k + \bar{D}r\end{aligned} \quad (39)$$

where
$$\bar{A}=\begin{bmatrix} A & 0 \\ -CA & I \end{bmatrix}, \bar{B}_1=\begin{bmatrix} B \\ -CB \end{bmatrix}, \bar{B}_2=\begin{bmatrix} 0 \\ -D \end{bmatrix}, \bar{F}_1=\begin{bmatrix} F \\ -CF \end{bmatrix},$$
$$\bar{F}_2=\begin{bmatrix} I \\ -C \end{bmatrix}, \bar{Z}=\begin{bmatrix} 0 \\ -Z \end{bmatrix}, \bar{H}=\begin{bmatrix} 0 \\ -I \end{bmatrix}, \bar{D}=\begin{bmatrix} 0 \\ I \end{bmatrix}.$$

Definition 1[22]: *Consider a system $x^+ = f(x,w)$ and a set $\Theta \subseteq \mathbb{R}^n$, if the system satisfies $x^+ = f(x,w) \in \Theta$ for any $x_0 \in \Theta$ and $w \in \Omega$, then Θ is called a robust invariant set of the system.* □

Definition 2[22]: *Consider the system $x^+ = f(x,w)$, and its robust invariant set $\Theta \subseteq X$ containing the origin as an interior point, if for any initial states $x_0 \in \Theta$ and $w \in \Omega$, there exists function α belonging to the class K_∞ and function β belonging to the class KL such that the system satisfies:*

$$\|\varphi(k;x_0,w)\| \le \beta(\|x_0\|,k) + \alpha(|w|), \forall k \in \mathbb{Z}_+ \quad (40)$$

Then the system is input to state stable (ISS) within Θ. □

Under Definition 2, it can be seen that when the system is not disturbed or only affected by attenuation disturbances, the system is finally asymptotically stable at the origin; when it is subjected to continuous bounded disturbances, the system is bounded and stable, and the final convergence range of the state trajectory is related to the upper bound of the continuous disturbances. On this basis, when the following Theorem 1 is satisfied, the gradient descent algorithm can be used to tune the output weight matrix, and then the compensation for random disturbances can be tuned gradually, which ensures the closed-loop control system under the disturbances has the input to state stability within the robust invariant set.

Theorem 1: *For the dynamic system described in Eqs.(1) and (2), if there exists constants $0 < \zeta, 0 < \upsilon < 1$ and $E\{\|\varepsilon_0\|^2\} \le \zeta^2$, making the following relationship satisfied:*

$$\|T_1\| = \upsilon$$
$$E\{[\|T_2\|\|w_k\| + \|T_3\|\|w_{k-1}\| + \|T_4\|\|v_k\| + \|T_5\|]^2\} \le (1-\upsilon)^2\zeta^2 \quad (41)$$

where:

$$\|T_1\| = \|\bar{A}\| + \|\bar{F}_2\|\|L_1\| + \|\bar{H}\|\|M_1\|, \|T_2\| = \|\bar{F}_1\|$$
$$\|T_3\| = \|\bar{F}_2\|\|L_3\| + \|\bar{H}\|\|M_3\|$$

$$\|T_4\| = \|\bar{Z}\| + \|\bar{H}\|\|L_6\|,$$
$$\|T_5\| = \|\bar{D}\|\|r\| + (\|\bar{H}\|\|M_2\| + \|\bar{B}_1\| + \|\bar{B}_2\| + \|\bar{F}_2\|\|L_2\|)v(W)$$

Then, under the En-NMPC control algorithm, the closed-loop control system under the disturbances described in Eqs.(1) and (2) has input-to-state stability within the robust invariant set.   □

Proof. See Appendix A.

B. Bounded Error of State Estimation

The accurate state estimation is the basis for the stable operation of the RBF network compensator of the proposed En-NMPC, so it is extremely important whether the EKF can track the states under the compensation. The stability of the filter is proved by analyzing the upper bound of the state estimation error. Under the condition of Assumption 3, the state estimation error is shown as follows:

$$
\begin{aligned}
\eta_k &= x_k - \hat{x}_k^+ \\
&= f(x_{k-1}, u_{k-1}, w_{k-1}) - f(\hat{x}_{k-1}^+, u_{k-1}, 0) - K_k(y_k - \hat{y}_k^-) \\
&= f(x_{k-1}, u_{k-1}, w_{k-1}) - f(\hat{x}_{k-1}^+, u_{k-1}, 0) \\
&\quad - K_k[h(x_k, u_k, v_k) - h(\hat{x}_k^-, u_k, 0)] \\
&\approx f(x_{k-1}, u_{k-1}, w_k) - f(\hat{x}_{k-1}^+, u_{k-1}, 0) \\
&\quad - K_k(Cx_k + Zv_k + \Delta h_k - C\hat{x}_k^- - \Delta h_{2k}) \\
&\approx (I - K_k C)[f(x_{k-1}, u_{k-1}, w_k) - f(\hat{x}_{k-1}^+, u_{k-1}, 0)] \\
&\quad - K_k(Zv_k + \Delta h_k - \Delta h_{2k})
\end{aligned}
\tag{42}
$$

On this basis, the EKF is stable under the En-NMPC algorithm when Theorem 2 is satisfied.

Theorem 2: *For the EKF used in the dynamic system described in Eqs.(1) and (2), if there are two constants $\upsilon > 0, \chi > 0$, which are satisfied with the following relationship:*

$$-\|I - K_k C\|\|L\| + \|K_k\|\|L_7\|\|L\| = \upsilon < 1 \tag{43}$$

$$\|K_k\|^2 \|Z\|^2 E\{\|v_k\|^2\} \le (1-\upsilon)^2 \chi^2 \tag{44}$$

$$\forall E\{\|\eta_0\|^2\} \le \chi^2 \tag{45}$$

Then, the state estimation error calculated by the EKF is bounded in the mean-square sense, under the proposed En-NMPC control algorithm.   □

Proof. See Appendix B.

V. CASE STUDY

The activated sludge wastewater treatment process (WWTP) as shown in Fig.2 mainly utilizes the microbial population in the activated sludge to adsorb, oxidize and decompose the organic matter in the sewage [23], [24]. Then through nitrification, denitrification, phosphorus release, phosphorus absorption, etc. to remove nitrogen and phosphorus pollutants. The quality of the WWTP depends on the two key factors in the sewage treatment: the nitrate concentration $D_{NO,2}$ in the second zone of the biochemical pool and the dissolved oxygen concentration $D_{O,5}$ in the fifth zone. Therefore, achieving high-performance and stable control of $D_{NO,2}$ and $D_{O,5}$ is the key issue in WWTP. The dissolved oxygen conversion coefficient $K_{La,5}$ of the fifth zone is generally adjusted by the blower to control $D_{O,5}$ in aerobic zone, and the return pump is used to adjust the internal flow Q_a to control $D_{NO,2}$ of the anoxic zone. However, due to the uncertainty and coupling of the biochemical
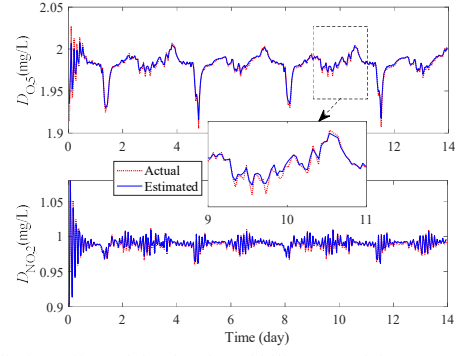

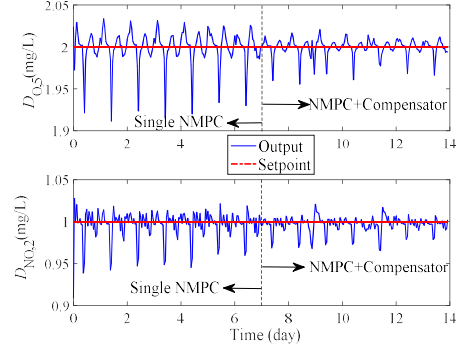**Fig.3** Prediction effect of the developed bilinear model

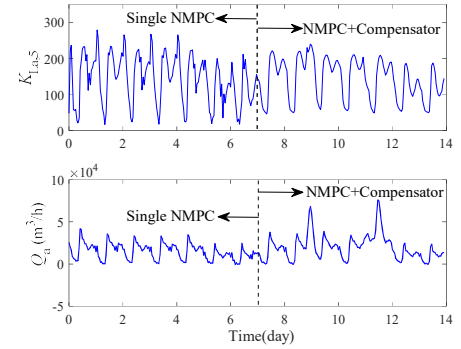**Fig.4** Control results with and without compensation

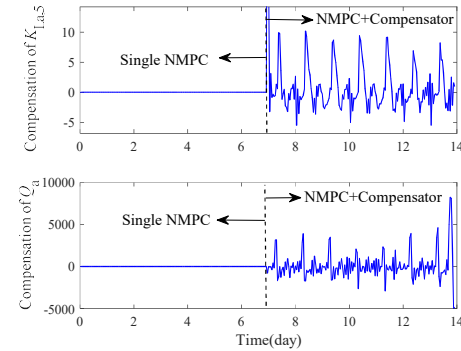**Fig.5** Changing curve of control input

Fig.6 Compensation of control input

reaction process, as well as the stochastic and non-stationary fluctuations of influent, the traditional predictive control method has poor control effect on the WWTP [24].

Here, the pre-denitrification process wastewater treatment benchmark platform BSM1 [24] is used as the simulation platform to fairly test the effectiveness and superiority of the proposed control method. BSM1 is currently the most important platform for evaluating the modeling and control methods for WWTP. In order to test the effect of the compensation of the algorithm when facing the stochastic non-stationary fluctuations, the experiments are carried out and based on the rainy-day conditions of WWTP.
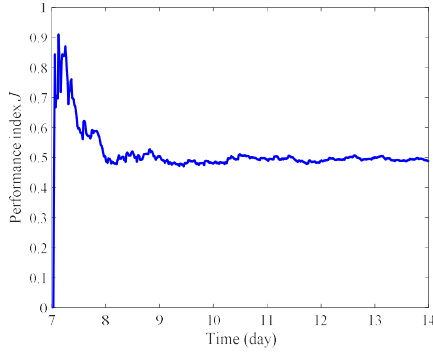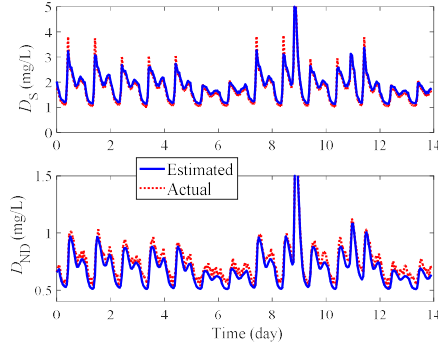
Fig.7 The curve of the performance index

Fig.8 States and its estimation by EKF

A. Control Experiment I

First, the bilinear state space model of the WWTP is obtained through the subspace identification in our previous work [23] as the prediction model in Problem 1. The main parameter matrices of the obtained prediction models are as follows:

$$A = \begin{bmatrix} 0.879 & \cdots & -0.012 \\ \vdots & \ddots & \vdots \\ 0.012 & \cdots & 0.822 \end{bmatrix}_{4\times4}, B = \begin{bmatrix} -0.056 & 0.056 \\ \vdots & \vdots \\ 0.019 & -0.010 \end{bmatrix}_{4\times2},$$

$$N = \begin{bmatrix} -0.0137 & \cdots & 0.0058 \\ \vdots & \ddots & \vdots \\ 0.0235 & \cdots & 0.0112 \end{bmatrix}_{4\times8},$$

$$C = \begin{bmatrix} -1.925 & \cdots & -0.693 \\ -1.884 & \cdots & 0.250 \end{bmatrix}_{2\times4}, D = \begin{bmatrix} 0.0792 & -0.0942 \\ 0.1149 & -0.0729 \end{bmatrix}$$

Fig.3 shows the prediction effect of the developed bilinear model. It can be seen that the subspace identification technology can effectively fit the changes in the sewage treatment process. Then, by taking the BSM1 platform as the controlled plant, the control experiment I of the proposed method is carried out as shown in Fig.2. In order to clearly demonstrate the effectiveness of the proposed method, only use the basic deterministic NMPC described in Eq.(8) to control during the first 7 days. After 7 days, the compensation controller described in Eq.(9) is added on the basis of NMPC which is a comparative control experiment with the first 7 days. In order to satisfy the convergence condition of the compensator described in Theorems 1 and 2, each parameter of performance index in Eq.(18) takes the value of R_1=0.7, R_2=1.3, R_3=0.6, R_4=0.4, η=0.001, and the prediction horizon and the control horizon are both N=15. The constraint of input Q_a is between 0 and 92230 m³/h, and the constraint of input $K_{La,5}$ is between 0 and 350. Moreover, the covariances of noises are selected as G_k=0.04 and Q_k=0.03. The number of center vectors in the RBF network hidden layer is selected as 3 by the Elbow algorithm. In order to find out which states have the largest relationship with $D_{O,5}$
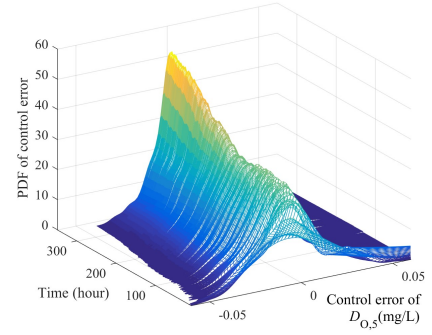

Fig.9 The evolution of control error PDF of $D_{O,5}$ and $D_{NO,2}$
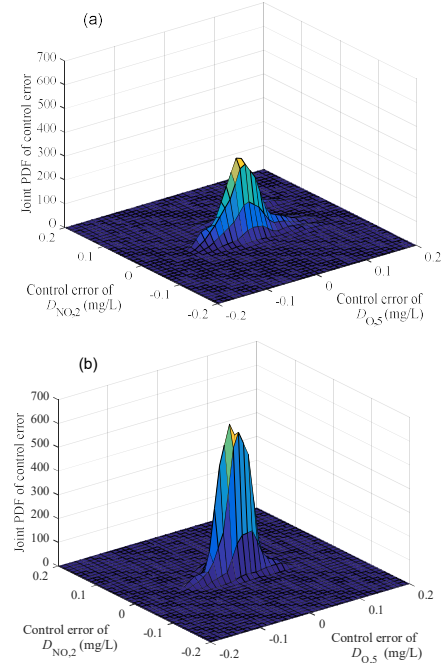

Fig.10 The (a) initial and (b) final joint-PDF of the two control errors

and $D_{NO,2}$, the canonical correlation analysis method is used to analyze the historical data. Finally, the concentration of soluble biodegradable organic matter D_S and degradable organic nitrogen D_{ND} are selected as the input of the compensator. These two states are also need to be estimated online by EKF.

Fig.4 and Fig.5 show the tracking control effects in rainy days with or without control compensation, Fig.6 shows the corresponding compensation of the control input Q_a and $K_{La,5}$ before and after the seventh day, and Fig.7 shows the change curve of the performance index about the control error entropy shown in Eq.(18) after adding the compensation control. It can be seen that the fluctuations of the control error of $D_{O,5}$ and $D_{NO,2}$ are significantly reduced after the proposed compensation is added to the basic control input, and the performance index used to measure the fluctuations of the
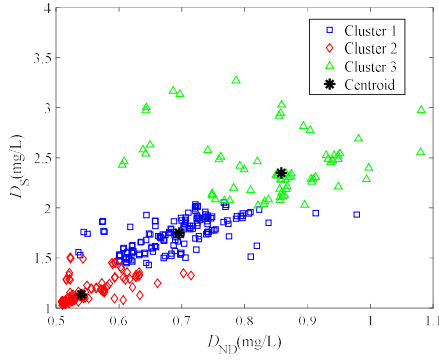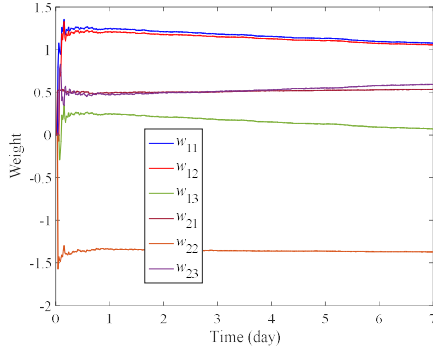
Fig.11 Cluster centers of historical input data

Fig.12 The adjustment process of output weights of compensator

Fig.13 Random changes of influent flowrate and the corresponding states in rainy days

Fig.14 Control results of WWTP under different control methods

control error gradually decreases until it converges to a smaller value. Moreover, Fig.8 is the online estimation curves of two states by EKF, which shows that the proposed method can obtain accurate estimation of the unknown states, so that the RBF network compensator based on this can keep stable all the time.

Fig.9 is the evolution trend of the PDF of the control error about $D_{O,5}$ and $D_{NO,2}$ after adding the compensation control. It can be seen that due to the compensation control, the PDF distribution of the control error changes from the original scattered and multi-peaked form to a more concentrated and single-peaked form. It can be seen from Fig.10 that after adding compensation input, the joint probability density function distribution of control error becomes more concentrated and the peak value is higher. This means that the compensation control effectively reduces the fluctuations of the control error of the basic deterministic NMPC and improves the control accuracy about $D_{O,5}$ and $D_{NO,2}$.

Fig.11 is the cluster centers of the input data obtained by the K-means clustering algorithm, which showing that the input data is divided into three categories. Fig.12 shows the process that the proposed method to correct the output weight matrix of the RBF network compensator by minimizing the performance index in Eq.(21). It can be seen that the weight matrix of the compensator tends to converge gradually, and under the influence of emergencies such as rainstorm, it tends to stable after only slight fluctuations.

B. Control Experiment II

During the actual production of WWTP, in order to ensure that the quality of the effluent reaches the standard while the energy consumption of operation is reduced at the same time, it is usually necessary to optimize and adjust the setpoint of output $D_{O,5}$ and $D_{NO,2}$ according to the changes of working conditions such as random changes of influent flowrate. Therefore, the influent flowrate is increased by 10% on the original basis during the 8th day and the 12th day which is
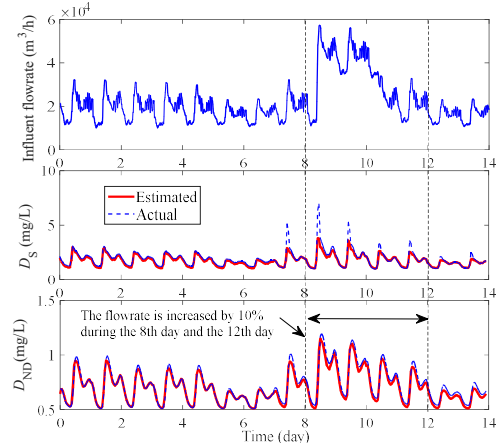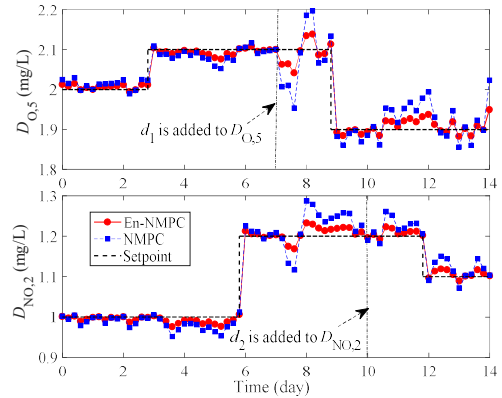
depicted between the dotted lines in Fig.13. Moreover, the proposed method is further tested for the control performance of the setpoint tracking with external random disturbances. Specifically, the step disturbances of d_1 and d_2, with 5% amplitude changes, are respectively added to $D_{O,5}$ and $D_{NO,2}$ after the 7th day and 10th day, and the durations are both 10h. The relevant parameters of the control system in this experiment are consistent with the previous Experiment I. As shown in Fig.13, due to the increase of the influent flowrate, both D_S and D_{ND} produce larger fluctuations between the dotted lines. However, the EKF in the proposed algorithm still achieves an accurate estimation of the states with only slight fluctuations.

Fig.14 shows the comparison of the control effect with different methods. It can be seen that under the basic deterministic NMPC method, there is a large control error between the actual output and their setpoints. However, the proposed En-NMPC effectively reduces the control error under disturbances. The output just has small and low-frequency fluctuations near the setpoints. Only when the setpoint changes and the disturbance enters, the actual $D_{O,5}$ and $D_{NO,2}$ produce small peak jitter, but through the rapid adjustment of the compensation control input, they quickly return to their respective setpoints. Therefore, the proposed En-NMPC method can effectively reduce the control error and significantly enhance the control performance by adding the compensation control input on the basic NMPC.

IV. CONCLUSION

For the multivariable stochastic dynamic systems, an enhanced NMPC (En-NMPC) method driven by control error compensation with entropy optimization and online

estimation of unknown states is proposed to solve the problem of insufficient performance of the existing deterministic NMPC. This method uses the EKF to obtain the posterior estimation of the unmeasured/unknown states as the input of the RBF network compensator. Under the optimization performance index constructed about the control error entropy, the output weight of the compensator is tuned to obtain the optimal compensation to the control input. The input-to-state stability of the system within a robust invariant set and the boundedness of the estimation error for EKF have been proved by the inductive reasoning method, which ensures the stability and the effect of the proposed method. Control experiments of sewage treatment process are designed, which fully verify the effectiveness and advancement of the proposed method.

APPENDIX A: PROOF OF THEOREM 1

Proof: Here, the inductive reasoning method is used to prove that all the states of the generalized system, depicted by Eq.(39), are bounded in the sense of the mean square value. Since the states of the designed generalized system are about the error and the integral of the error, the input-to-state stability of the system with respect to disturbances is further proved by extension that under the proposed En-NMPC algorithm. Then, on the basis of Assumption 4 and Lemma 1 and 2, substituting Eqs.(32) and (34) into Eq.(39), we can get:

$$
\begin{aligned}
&E\{\varepsilon_1^{\mathrm{T}}\varepsilon_1\} \\
&= E\{(\bar{A}\varepsilon_0 + \bar{B}_1 u_0 + \bar{B}_2 u_1 + \bar{F}_1 w_1 + \bar{F}_2 \Delta f_0 + \bar{Z}v_1 + \bar{H}\Delta h_1 + \bar{D}r)^{\mathrm{T}} \\
&\quad (\bar{A}\varepsilon_0 + \bar{B}_1 u_0 + \bar{B}_2 u_1 + \bar{F}_1 w_1 + \bar{F}_2 \Delta f_0 + \bar{Z}v_1 + \bar{H}\Delta h_1 + \bar{D}r)\} \\
&\leq (\|\bar{A}\| + \|\bar{F}_2\|\|L_1\| + \|\bar{H}\|\|M_1\|)^2 E\{\|\varepsilon_0\|^2\} \\
&\quad + E\{[\|\bar{F}_1\|\|w_1\| + (\|\bar{F}_2\|\|L_3\| + \|\bar{H}\|\|M_3\|)\|w_0\| \\
&\quad + (\|\bar{Z}\| + \|\bar{H}\|\|L_6\|)\|v_1\| + \|\bar{D}\|r \\
&\quad + (\|\bar{H}\|\|M_2\| + \|\bar{B}_1\| + \|\bar{B}_2\| + \|\bar{F}_2\|\|L_2\|)\nu(W)]^2\} \\
&\quad + 2(\|\bar{A}\| + \|\bar{F}_2\|\|L_1\| + \|\bar{H}\|\|M_1\|)E\{\|\varepsilon_0\|\}E\{[\|\bar{F}_1\|\|w_1\| \\
&\quad + (\|\bar{F}_2\|\|L_3\| + \|\bar{H}\|\|M_3\|)\|w_0\| + (\|\bar{Z}\| + \|\bar{H}\|\|L_6\|)\|v_1\| + \|\bar{D}\|r \\
&\quad + (\|\bar{H}\|\|M_2\| + \|\bar{B}_1\| + \|\bar{B}_2\| + \|\bar{F}_2\|\|L_2\|)\nu(W)]\} \\
&\leq \|T_1\|^2 E\{\|\varepsilon_0\|^2\} + E\{[\|T_2\|\|w_1\| + \|T_3\|\|w_0\| + \|T_4\|\|v_1\| + \|T_5\|]^2\} \\
&\quad + 2\|T_1\|E\{\|\varepsilon_0\|\}E\{[\|T_2\|\|w_1\| + \|T_3\|\|w_0\| + \|T_4\|\|v_1\| + \|T_5\|]\} \\
&< \zeta^2 \upsilon^2 + (1-\upsilon)^2 \zeta^2 + 2\zeta^2 \upsilon(1-\upsilon) \\
&= \zeta^2
\end{aligned}
\tag{46}
$$

Therefore, there is a constant τ_1 such that:

$$
E\{\varepsilon_1^{\mathrm{T}}\varepsilon_1\} \leq \tau_1^2 \zeta^2
$$

It can be seen from the above that at time $k=1$, the upper bound of the state of the generalized system Eq.(39) is $\tau_1^2 \zeta^2$ in the sense of the mean square. To further analyze the input-to-state stability of the algorithm against disturbances, the terms of the last inequality in Eq.(46) are analyzed in detail. Due to $0 < T_1 < 1$ and combined with Eq.(41), it can be known that there must be a function $\beta(\cdot,\cdot)$ which is belonging to the class KL function that satisfies:

$$
\begin{aligned}
\|T_1\|^2 E\{\|\varepsilon_0\|^2\} + 2\|T_1\|E\{\|\varepsilon_0\|\}E\{[\|T_2\|\|w_1\| + \|T_3\|\|w_0\| \\
+ \|T_4\|\|v_1\| + \|T_5\|]\} \leq \beta(\|\varepsilon_0\|, 1)
\end{aligned}
\tag{47}
$$

At the same time, it can be seen from Eq.(41) that there is a function $\alpha(|w|)$ which is belonging to the class K_∞ function that satisfies:

$$
E\{[\|T_2\|\|w_1\| + \|T_3\|\|w_0\| + \|T_4\|\|v_1\| + \|T_5\|]^2\} \leq \alpha(|w|)
\tag{48}
$$

Combining Eqs.(47) and (48), it can be known that there is an upper bound in the mean square sense for its state of the generalized system $\varphi(k; \varepsilon_0, w)$ at time k:

$$
\|\varphi(1; \varepsilon_0, w)\| \leq \beta(\|\varepsilon_0\|, k) + \alpha(|w|)
\tag{49}
$$

Further, at time $k=2$, there exists:

$$
\begin{aligned}
&E\{\varepsilon_2^{\mathrm{T}}\varepsilon_2\} \\
&= E\{(\bar{A}\varepsilon_1 + \bar{B}_1 u_1 + \bar{B}_2 u_2 + \bar{F}_1 w_2 + \bar{F}_2 \Delta f_1 + \bar{Z}v_2 + \bar{H}\Delta h_2 + \bar{D}r)^{\mathrm{T}} \\
&\quad (\bar{A}\varepsilon_1 + \bar{B}_1 u_1 + \bar{B}_2 u_2 + \bar{F}_1 w_2 + \bar{F}_2 \Delta f_1 + \bar{Z}v_2 + \bar{H}\Delta h_2 + \bar{D}r)\} \\
&\leq (\|\bar{A}\| + \|\bar{F}_2\|\|L_1\| + \|\bar{H}\|\|M_1\|)^2 E\{\|\varepsilon_1\|^2\} \\
&\quad + E\{[\|\bar{F}_1\|\|w_2\| + (\|\bar{F}_2\|\|L_3\| + \|\bar{H}\|\|M_3\|)\|w_1\| \\
&\quad + (\|\bar{Z}\| + \|\bar{H}\|\|L_6\|)\|v_2\| + \|\bar{D}\|r \\
&\quad + \|\bar{H}\|\|M_2\| + (\|\bar{B}_1\| + \|\bar{B}_2\| + \|\bar{F}_2\|\|L_2\|)\nu(W)]^2\} \\
&\quad + 2(\|\bar{A}\| + \|\bar{F}_2\|\|L_1\| + \|\bar{H}\|\|M_1\|)E\{\|\varepsilon_1\|\}E\{[\|\bar{F}_1\|\|w_2\| \\
&\leq \|T_1\|^2 E\{\|\varepsilon_1\|^2\} + E\{[\|T_2\|\|w_2\| + \|T_3\|\|w_1\| + \|T_4\|\|v_2\| + \|T_5\|]^2\} \\
&\quad + 2\|T_1\|E\{\|\varepsilon_1\|\}E\{[\|T_2\|\|w_2\| + \|T_3\|\|w_1\| + \|T_4\|\|v_2\| + \|T_5\|]\} \\
&\quad + (\|\bar{F}_2\|\|L_3\| + \|\bar{H}\|\|M_3\|)\|w_1\| + (\|\bar{Z}\| + \|\bar{H}\|\|L_6\|)\|v_2\| + \|\bar{D}\|r \\
&\quad + \|\bar{H}\|\|M_2\| + \|\bar{B}_1\| + \|\bar{B}_2\| + \|\bar{F}_2\|\|L_2\|)\nu(W)]\} \\
&< \tau_1^2 \zeta^2 \upsilon^2 + (1-\upsilon)^2 \zeta^2 + 2\tau_1 \zeta^2 \upsilon(1-\upsilon) \\
&= [\tau_1 \upsilon + (1-\upsilon)]^2 \zeta^2
\end{aligned}
\tag{50}
$$

In the same way, there is a constant τ_2 such that the following inequality holds: $E\{\varepsilon_2^{\mathrm{T}}\varepsilon_2\} \leq \tau_2^2[\tau_1\upsilon + (1-\upsilon)]^2 \zeta^2$.

Further analysis the terms in Eq.(50) at time $k=2$. Due to $0 < T_1 < 1$, Eq.(51) has a decreasing relationship with respect to Eq. (47), so the function $\beta(\cdot,\cdot)$ still satisfies the following inequality:

$$
\begin{aligned}
\|T_1\|^2 E\{\|\varepsilon_1\|^2\} + 2\|T_1\|E\{\|\varepsilon_1\|\}E\{[\|T_2\|\|w_2\| \\
+ \|T_3\|\|w_1\| + \|T_4\|\|v_2\| + \|T_5\|]\} \leq \beta(\|\varepsilon_0\|, 2)
\end{aligned}
\tag{51}
$$

In the same way, $\alpha(|w|)$ which is belonging to the class K_∞ function still satisfies the following inequality:

$$
E\{[\|T_2\|\|w_2\| + \|T_3\|\|w_1\| + \|T_4\|\|v_2\| + \|T_5\|]^2\} \leq \alpha(|w|)
\tag{52}
$$

Which is $\|\varphi(2; \varepsilon_0, w)\| \leq \beta(\|\varepsilon_0\|, 2) + \alpha(|w|)$.

Suppose that when at time $k \geq 2$, there always exists:

$$
E\{\varepsilon_k^{\mathrm{T}}\varepsilon_k\} \leq \tau_k^2 T_k^2 \zeta^2, 0 < \tau_k < 1, k \geq 2
\tag{53}
$$

where

$$
T_k^2 = (\sum_{i=1}^{k-1}\tilde{\tau}_{ki} - \upsilon\sum_{i=1}^{k-2}\tilde{\tau}_{ki} + 1 - \upsilon)^2, \ \tilde{\tau}_{ki} = \upsilon^i \prod_{n=1}^{i}\tau_{k-n}.
$$

Further, at time $k+1$, it can be known that:

$$
\begin{aligned}
&E\{\varepsilon_{k+1}^{\mathrm{T}}\varepsilon_{k+1}\} = \\
&E\{(\bar{A}\varepsilon_k + \bar{B}_1 u_k + \bar{B}_2 u_{k+1} + \bar{F}_1 w_{k+1} + \bar{F}_2 \Delta f_k + \bar{Z}v_{k+1} + \bar{H}\Delta h_{k+1} + \bar{D}r)^{\mathrm{T}} \\
&(\bar{A}\varepsilon_k + \bar{B}_1 u_k + \bar{B}_2 u_{k+1} + \bar{F}_1 w_{k+1} + \bar{F}_2 \Delta f_k + \bar{Z}v_{k+1} + \bar{H}\Delta h_{k+1} + \bar{D}r)\} \\
&\leq (\|\bar{A}\| + \|\bar{F}_2\|\|L_1\| + \|\bar{H}\|\|M_1\|)^2 E\{\|\varepsilon_k\|^2\} + E\{[\|\bar{F}_1\|\|w_{k+1}\|
\end{aligned}
$$

$$+(\|\bar{F}_2\|\|L_3\|+\|\bar{H}\|\|M_3\|)\|w_k\|+(\|\bar{Z}\|+\|\bar{H}\|\|L_6\|)\|v_{k+1}\|$$
$$+\|\bar{D}\|r+\|\bar{H}\|\|M_2\|+(\|\bar{B}_1\|+\|\bar{B}_2\|+\|\bar{F}_2\|\|L_2\|)\nu(W)]^2\}$$
$$+2(\|\bar{A}\|+\|\bar{F}_2\|\|L_1\|+\|\bar{H}\|\|M_1\|)E\{\varepsilon_k\}E\{[\|\bar{F}_1\|\|w_{k+1}\|$$
$$+(\|\bar{F}_2\|\|L_3\|+\|\bar{H}\|\|M_3\|)\|w_k\|+(\|\bar{Z}\|+\|\bar{H}\|\|L_6\|)\|v_{k+1}\|+\|\bar{D}\|r$$
$$+(\|\bar{H}\|\|M_2\|+\|\bar{B}_1\|+\|\bar{B}_2\|+\|\bar{F}_2\|\|L_2\|)\nu(W)]\}$$
$$\leq\|T_1\|^2 E\{\|\varepsilon_k\|^2\}$$
$$+E\{[\|T_2\|\|w_{k+1}\|+\|T_3\|\|w_k\|+\|T_4\|\|v_{k+1}\|+\|T_5\|]^2\}$$
$$+2\|T_1\|E\{\varepsilon_k\}E\{[\|T_2\|\|w_{k+1}\|+\|T_3\|\|w_k\|+\|T_4\|\|v_{k+1}\|+\|T_5\|]\}$$
$$<\upsilon^2\tau_k^2 T_k^2\zeta^2+2\tau_k T_k\upsilon(1-\upsilon)\zeta^2+(1-\upsilon)^2\zeta^2$$
$$=[\upsilon\tau_k T_k+(1-\upsilon)]^2\zeta^2$$

(54)

There is always a constant $\tau_{k+1}, 0<\tau_{k+1}<1$, such that the following inequality holds:

$$E\{\varepsilon_{k+1}^T\varepsilon_{k+1}\}\leq\tau_{k+1}^2[\upsilon\tau_k T_k+(1-\upsilon)]^2\zeta^2.$$

Therefore, when the condition of Eq.(41) is satisfied at time k, the mean of the estimation error at time $k+1$ is always less than a constant. when iterating from the initial state ε_0 with $k\to\infty$, the left term in Eq.(55) decreases monotonically and tends to zero, due to $0\leq\|T_1\|\leq1$, then $\beta(\|\varepsilon_0\|,k+1)$ still satisfies the following relationship:

$$\|T_1\|^2 E\{\|\varepsilon_k\|^2\}+2\|T_1\|E\{\varepsilon_k\}E\{[\|T_2\|\|w_{k+1}\|$$
$$+\|T_3\|\|w_k\|+\|T_4\|\|v_{k+1}\|+\|T_5\|]\}\leq\beta(\|\varepsilon_0\|,k+1)$$

(55)

Similarly, $\alpha(\cdot)$ which is belonging to the class K_∞ still satisfies the following inequality:

$$E\{[\|T_2\|\|w_{k+1}\|+\|T_3\|\|w_k\|+\|T_4\|\|v_{k+1}\|+\|T_5\|]^2\}\leq\alpha(|w|) \quad (56)$$

Which is $\|\varphi(k+1;\varepsilon_0,w)\|\leq\beta(\|\varepsilon_0\|,k+1)+\alpha(|w|)$, this means that Theorem 1 is proved.

APPENDIX B: PROOF OF THEOREM 2

Proof. The stability of the EKF is proved by analyzing the boundedness of the estimation error of the state. Under the condition of Assumption 3, the estimation error of the state is depicted by Eq.(42), so it can be further known that:

$$\eta_k^T\eta_k$$
$$\approx[(I-K_k C)(f(x_{k-1},u_{k-1},w_k)-f(\hat{x}_{k-1}^+,u_{k-1},0))$$
$$-K_k(Zv_k+\Delta h_k-\Delta h_{2k})]^T$$
$$[(I-K_k C)(f(x_{k-1},u_{k-1},w_k)-f(\hat{x}_{k-1}^+,u_{k-1},0))$$
$$-K_k(Zv_k+\Delta h_k-\Delta h_{2k})]$$
$$\approx[(I-K_k C)(f(x_{k-1},u_{k-1},w_k)-f(\hat{x}_{k-1}^+,u_{k-1},0)) \quad (57)$$
$$-K_k(\Delta h_k-\Delta h_{2k})]^T$$
$$[(I-K_k C)(f(x_{k-1},u_{k-1},w_k)-f(\hat{x}_{k-1}^+,u_{k-1},0))$$
$$-K_k(\Delta h_k-\Delta h_{2k})]$$
$$+(K_k Zv_k)^T K_k Zv_k-2[(I-K_k C)\times(f(x_{k-1},u_{k-1},w_k)$$
$$-f(\hat{x}_{k-1}^+,u_{k-1},0))-K_k(\Delta h_k-\Delta h_{2k})]^T K_k Zv_k$$

On the basis of Assumptions 2 and 3, there is an upper bound of the estimation error at time $k=1$, which satisfies the following inequality:

$$E\{\eta_1^T\eta_1\}$$
$$\approx E\{[(I-K_1 C)(f(x_0,u_0,w_1)-f(\hat{x}_0^+,u_0,0))-K_1(\Delta h_1-\Delta h_{2_1})]^T$$
$$\times[(I-K_1 C)(f(x_0,u_0,w_1)-f(\hat{x}_0^+,u_0,0))-K_1(\Delta h_1-\Delta h_{2_1})]$$
$$-2[(I-K_1 C)(f(x_0,u_0,w_1)-f(\hat{x}_0^+,u_0,0))-K_1(\Delta h_1-\Delta h_{2_1})]^T$$
$$\times K_1 Zv_1+(K_1 Zv_1)^T K_1 Zv_1\}$$
$$\leq(\|I-K_1 C\|\|L\|-\|K_1\|\|L_7\|)^2 E\{\eta_0^2\}+\|K_1\|^2\|Z\|^2 E\{v_1^2\}$$
$$-2(\|I-K_1 C\|\|L\|-\|K_1\|\|L_7\|)E\{\eta_0\}\|K_1\|\|Z\|E\{v_1\}$$
$$\leq\upsilon^2\chi^2+(1-\upsilon)^2\chi^2+2\upsilon(1-\upsilon)\chi^2=\chi^2$$

(58)

There always exists constant $\bar{\tau}_1, 0<\bar{\tau}_1<1$ such that

$$E\{\eta_1^T\eta_1\}\leq\bar{\tau}_1^2\chi^2 \quad (59)$$

At time $k=2$, the estimation error is similarly analyzed to find that:

$$E\{\eta_2^T\eta_2\}$$
$$\approx E\{[(I-K_2 C)$$
$$\times(f(x_1,u_1,w_2)-f(\hat{x}_1^+,u_1,0))-K_2(\Delta h_2-\Delta h_{22})]^T$$
$$\times[(I-K_2 C)(f(x_1,u_1,w_2)-f(\hat{x}_1^+,u_1,0))-K_2(\Delta h_2-\Delta h_{22})]$$
$$+(K_2 Zv_2)^T K_2 Zv_2-2[(I-K_2 C)(f(x_1,u_1,w_2)-f(\hat{x}_1^+,u_1,0))$$
$$-K_2(\Delta h_2-\Delta h_{22})]^T K_2 Zv_2\}$$
$$\leq(-\|I-K_2 C\|\|L\|+\|K_2\|\|L_7\|)^2 E\{\eta_1^2\}$$
$$+\|K_2\|^2\|Z\|^2 E\{v_2^2\}$$
$$+2(-\|I-K_2 C\|\|L\|+\|K_2\|\|L_7\|)E\{\eta_1\}\|K_2\|\|Z\|E\{v_2\}$$
$$\leq\upsilon^2\bar{\tau}_1^2\chi^2+(1-\upsilon)^2\chi^2+2\upsilon(1-\upsilon)\bar{\tau}_1\chi^2$$
$$=[\bar{\tau}_1\upsilon+(1-\upsilon)]^2\chi^2$$

(60)

There always exists $\bar{\tau}_2, 0<\bar{\tau}_2<1$ such that

$$E\{\eta_2^T\eta_2\}\leq\bar{\tau}_2^2[\bar{\tau}_1\upsilon+(1-\upsilon)]^2\chi^2 \quad (61)$$

Suppose the following inequality exists at time $k\geq2$:

$$E(\eta_k^T\eta_k)\leq\bar{\tau}_k^2\bar{\Upsilon}_k^2\chi^2, 0<\bar{\tau}_k<1 \quad (62)$$

where $\begin{cases}\bar{\Upsilon}_k^2=(\sum_{i=1}^{k-1}\tau_{k_i}^{\approx}-\upsilon\sum_{i=1}^{k-2}\tau_{k_i}^{\approx}+1-\upsilon)^2 \\ \tau_{k_i}^{\approx}=\upsilon^i\prod_{n=1}^i\bar{\tau}_{k-n}\end{cases}$.

Then when at time $k+1$, the upper limit of the estimation error satisfies the following inequality:

$$E(\eta_{k+1}^T\eta_{k+1})\leq(-\|I-K_{k+1}C\|\|L\|+\|K_{k+1}\|\|L_7\|)^2 E\{\eta_k^2\}$$
$$+\|K_{k+1}\|^2\|Z\|^2 E\{v_{k+1}^2\}$$
$$+2(-\|I-K_{k+1}C\|\|L\|+\|K_{k+1}\|\|L_7\|) \quad (63)$$
$$\times E\{\eta_k\}\|K_{k+1}\|\|Z\|E\{v_{k+1}\}$$

Further, we can obtain:

$$E(\eta_{k+1}^T\eta_{k+1})\leq\upsilon^2\bar{\tau}_k^2\bar{\Upsilon}_k^2\chi^2+(1-\upsilon)^2\chi^2+2\upsilon(1-\upsilon)\bar{\tau}_k\bar{\Upsilon}_k\chi^2$$
$$=[\bar{\tau}_k\bar{\Upsilon}_k\upsilon+(1-\upsilon)]^2\chi^2$$

Therefore, based on the above inequality, there is always a constant $\bar{\tau}_{k+1}$ that makes the following equation true:

$$E(\eta_{k+1}^T\eta_{k+1})\leq\bar{\tau}_{k+1}^2[\bar{\tau}_k\bar{\Upsilon}_k\upsilon+(1-\upsilon)]^2\chi^2=\bar{\tau}_{k+1}^2\bar{\Upsilon}_{k+1}^2\chi^2 \quad (64)$$

That is, the estimation error always has a finite upper bound in the mean square sense, thus Theorem 2 is proved.

REFERENCES

[1] D.Q. Mayne, "Model predictive control: recent developments and future promise," *Automatica*, vol.50, pp.2967–2986, Dec. 2014.

[2] P. Zhou, H. D. Song, H. Wang, and T. Y. Chai, "Data-driven nonlinear subspace modeling for prediction and control of molten iron quality indices in blast furnace ironmaking," *IEEE Trans. Control Systems Technology*, vol.25, no.5, pp.1761–1774, Dec. 2016.

[3] J. Berberich, J. Köhler, M.A. Müller, and F. Allgöwer, "Data-driven model predictive control with stability and robustness guarantees," *IEEE Trans. Autom. Control*, vol. 66, no. 4, pp. 1702–17, Jun 2020.

[4] L. Hewing, J. Kabzan, and M. N Zeilinger, "Cautious model predictive control using Gaussian process regression," *IEEE Trans. Control Systems Technology*, vol.28, no.6, pp.2736–2743, Nov. 2019.

[5] D.Q. Mayne, J.B. Rawlings, C.V. Rao, and P.O.M. Scokaert, "Constrained model predictive control: stability and optimality," *Automatica*, vol.36, no.6, pp.789–814, Jun 2000.

[6] D. Limon, I. Alvarado, T. Alamo, and E.F. Camacho, "Robust tube-based MPC for tracking of constrained linear systems with additive disturbances," *J. Process Control*, vol. 20, pp. 248–260, Mar. 2010.

[7] M. Cannona, Q.F. Cheng, B. Kouvaritakis, and S.V. Raković, "Stochastic tube MPC with state estimation," *Automatica*, vol. 48, pp. 536–541, Mar. 2012.

[8] C. Liu, H. Li, J. Gao, and D. Xu, "Robust self-triggered min-max model predictive control for discrete-time nonlinear systems," *Automatica*, vol. 89, pp. 333–339, Mar. 2018.

[9] B. T. Lopez, J. E. Slotine, and J. P. How, "Dynamic Tube MPC for Nonlinear Systems," *2019 American Control Conference (ACC)*, Philadelphia, PA, USA, 2019, pp. 1655–1662.

[10] G. C. Calafiore and M. C. Campi, "The scenario approach to robust control design," *IEEE Trans. Autom. Control*, vol.51, no.5, pp. 742–753, May 2006.

[11] H. Chen and F. Allgöwer, "A quasi-infinite horizon nonlinear model predictive control scheme with guaranteed stability," *Automatica*, vol.34, no.10, pp.1205–1217, Oct. 1998.

[12] B.R. Maner, J. Francis, I. Doyle, B. A. Ogunnaike, and R. K. Pearson, "Nonlinear model predictive control of a simulated multivariable polymerization reactor using second-order volterra models," *Automatica*, vol. 32, no. 9, pp. 1285–1301, Sep. 1996.

[13] Y. Yi, W. X. Zheng, C. Y. Sun, and L. Guo, "DOB fuzzy controller design for non- Gaussian stochastic distribution systems using two-step fuzzy identification," *IEEE Trans. Fuzzy Systems*, vol.24, no.2, pp, 401–418, Jul. 2016.

[14] Q. C. Zhang and H. Wang, "A novel data-based stochastic distribution control for non-Gaussian stochastic systems," *IEEE Trans. Autom. Control*, vol. 67, no.3, pp. 1506–1513, Mar. 2022.

[15] Y.Y. Zhou, A.P. Wang, P. Zhou, H. Wang, and T.Y. Chai, "Dynamic performance enhancement for nonlinear stochastic systems using RBF driven nonlinear compensation with extended Kalman filter," *Automatica*, vol. 112, pp. 1–15, Jun. 2020.

[16] X. Yin, Q. C. Zhang, H. Wang, and Z. Ding, "RBFNN-based minimum entropy filtering for a class of stochastic nonlinear systems," *IEEE Trans. Automatic Control*, vol.65, no.1, pp.376–381, May 2019.

[17] J. F. Qiao and H. G. Han, "Identification and modeling of nonlinear dynamical systems using a novel self-organizing RBF-based approach," *Automatica*, vol.48, no.8, pp.1729–1734, Aug. 2012.

[18] F. Liu and Y. Deng, "Determine the number of unknown targets in Open World based on Elbow method," *IEEE Trans. Fuzzy Systems*, vol. 29, no.5, pp. 986–995, Jan. 2020.

[19] Y.Y. Zhou, Q. Zhang, H. Wang, P. Zhou, and T.Y. Chai, "EKF-based enhanced performance controller design for nonlinear stochastic systems," *IEEE Trans. Automatic Control*, vol.63, no.4, pp.1155–1162, Aug. 2018.

[20] L. P. Yin and L. Guo, "Fault isolation for dynamic multivariate nonlinear non-Gaussian stochastic systems using generalized entropy optimization principle," *Automatica*, vol. 45, pp. 2612–2619, 2009.

[21] M. Ababneh, M. Salah, and K. Alwidyan, "Linearization of nonlinear dynamical systems: a comparative study," *Jordan J. Mech. & Ind. Eng.*, vol. 5, no. 6, pp. 567–571, Dec. 2011.

[22] L. Magni, D.M. Raimondo, and R. Scattolini, "Regional input-to-state stability for nonlinear model predictive control," *IEEE Trans. Automatic Control*, vol. 51, no. 9, pp. 1548−1553, Sep.2006.

[23] S. Zhang, P. Zhou, Y. F. Xie, and T. Y. Chai, "Improved model-free adaptive predictive control method for direct data-driven control of a wastewater treatment process with high performance," *J. Process Control*, vol. 110, pp. 11–23, Feb. 2022.

[24] J. F. Qiao, Y. Hou, and H. G. Han, "Optimal control for wastewater treatment process based on an adaptive multi-objective differential evolution algorithm," *Neural Comput. Appl.*, vol.31, no.1, pp.2537–2550, Jul. 2019.

Ping Zhou (M'12–SM'17) received the B.S., M.S., and Ph.D. degrees in control theory and engineering from Northeastern University, in 2003, 2006, and 2013, respectively. He has worked in Northeastern University since 2010. He is currently a Professor with the State Key Laboratory of Synthetical Automation for Process Industries, Northeastern University. His research interests include feedback control for optimal process operation, and data-driven modeling, monitoring and control with various industrial applications. He has authored 2 monographs and more than 100 referred journal publications in these areas.

Dr. Zhou won the First Prize of Natural Science Award of Chinese Association of Automation in 2021 and the Second Prize of Natural Science Award of the Ministry of Education of China in 2020. He also received the Rockwell Automation Award for the Outstanding Application Paper of the Six World Congress on Intelligent Control and Automation in 2006. He was a recipient of the Top Young Talents Award of the National Ten Thousand Talents Plan of China in 2019. He currently serves as a lead guest editor of the IEEE TRANSACTIONS ON AUTOMATION SCIENCE AND ENGINEERING for the Special Issue on Learning from Imperfect Data for Industrial Automation, and a lead guest editor of the *Journal of Control Theory and Applications* for the Special Issue on AI-Driven Automation and Intellectualization of Process Industry.

Sun Xiaoyang received the B.S. degree in Automation from Jiangsu University of Science and Technology, Zhenjiang, China, in 2019.

He is currently pursuing the Ph.D degree in the State Key Laboratory of Synthetical Automation for Process Industries, Northeastern University, Shenyang, China. His research interest is event-triggered control and model predictive control.

Tianyou Chai (F'07) received the Ph.D. degree in control theory and engineering in 1985 from Northeastern University, Shenyang, China, where he became a Professor in 1988. He is the founder and Director of the Center of Automation, which became a National Engineering and Technology Research Center and a State Key Laboratory. He is a member of Chinese Academy of Engineering, IFAC Fellow and IEEE Fellow.

His current research interests include modelling, control, optimization and integrated automation of complex industrial processes. He has published 230 peer reviewed international journal papers. His paper titled Hybrid intelligent control for optimal operation of shaft furnace roasting process was selected as one of three best papers for the Control Engineering Practice Paper Prize for 2011-2013. He has developed control technologies with applications to various industrial processes. For his contributions, he has won 4 prestigious awards of National Science and Technology Progress and National Technological Innovation, the 2007 Industry Award for Excellence in Transitional Control Research from IEEE Multiple-conference on Systems and Control, and the 2017 Wook Hyun Kwon Education Award from Asian Control Association.